



# Journal of Applied Sciences

ISSN 1812-5654

**science**  
alert

**ANSI***net*  
an open access publisher  
<http://ansinet.com>

## A Numerical Simulation of Wind-induced Flows in Ariake Sea

<sup>1</sup>M. Abualtayef, <sup>1</sup>M. Kuroiwa, <sup>1</sup>K. Tanaka, <sup>1</sup>Y. Matsubara and <sup>2</sup>J. Nakahira

<sup>1</sup>Department of Civil Engineering, Tottori University, Tottori, Japan

<sup>2</sup>Yachiyo Consulting Engineers, Tokyo Shinjukuku Nishiotiai, Japan

**Abstract:** A new development of a three dimensional (3D) multi-layer wind-induced circulation model of Ariake Sea region is described in this study. The hydrodynamic equations are derived from 3D Navier Stokes equations and solved using the Fractional Step Method (FSM). The 3D hydrodynamic model is first tested against analytical solution in order to investigate the performance of the model. And then, it was applied to the Ariake Sea. For model test, the numerical results are almost identical to the analytical solutions. It was shown that the numerical model developed was capable to simulate wind-induced flows in shallow semi-enclosed/enclosed waters.

**Key words:** Wind-induced circulations, fractional step method, Ariake sea

### INTRODUCTION

The development of numerical model for wind-induced flows in coastal areas is essential in determining the fate of water quality problems such as oil spills (Elliott, 1986) and heavy metals adhering to sediments (Huntley and Bowen, 1990). During the past few decades, several 3D circulation models have been developed, for example, those of Heaps (1972), Koutitas and Gousidou-Koutita (1986), Davies and Jones (1992), Casulli and Cheng (1992), Jin and Kranenburg (1993), Caviglia and Dragani (1996), Huai *et al.* (2003) and Kocyigit and Kocyigit (2004). By using FSM model with a regular fixed grid, the model is able to resolve complicated topographic features, with good vertical resolution in extremely shallow sea areas.

The aim of this study was to develop a 3D numerical model to clarify the circulation patterns over a complex bathymetry in semi-enclosed/enclosed waters.

### MATHEMATICAL DESCRIPTION

**Governing equations:** The 3D non-linear hydrodynamic Equations in Cartesian coordinates are:

$$\frac{\partial u}{\partial x} + \frac{\partial v}{\partial y} + \frac{\partial w}{\partial z} = 0 \quad (1)$$

$$\frac{\partial u}{\partial t} = fv - u \frac{\partial u}{\partial x} - v \frac{\partial u}{\partial y} - w \frac{\partial u}{\partial z} - g \frac{\partial \eta}{\partial x}$$

$$+ \frac{\partial}{\partial x} \left( \epsilon_h \frac{\partial u}{\partial x} \right) + \frac{\partial}{\partial y} \left( \epsilon_h \frac{\partial u}{\partial y} \right) + \frac{\partial}{\partial z} \left( \epsilon_v \frac{\partial u}{\partial z} \right) \quad (2)$$

$$\frac{\partial v}{\partial t} = -fu - u \frac{\partial v}{\partial x} - v \frac{\partial v}{\partial y} - w \frac{\partial v}{\partial z} - g \frac{\partial \eta}{\partial y} + \frac{\partial}{\partial x} \left( \epsilon_h \frac{\partial v}{\partial x} \right) + \frac{\partial}{\partial y} \left( \epsilon_h \frac{\partial v}{\partial y} \right) + \frac{\partial}{\partial z} \left( \epsilon_v \frac{\partial v}{\partial z} \right) \quad (3)$$

$$w = w_{z=h} - \frac{\partial}{\partial x} \int_{-h}^z u dz - \frac{\partial}{\partial y} \int_{-h}^z v dz \quad (4)$$

$$\frac{\partial \eta}{\partial t} = - \frac{\partial}{\partial x} \int_{-h}^{\eta} u dz - \frac{\partial}{\partial y} \int_{-h}^{\eta} v dz \quad (5)$$

where:

- u, v, w Cartesian velocity components along axis x, y and z, respectively;
- h Water depth;
- $\eta$  Free surface water elevation above the water depth;
- g Acceleration of gravity;
- t Time;
- f Coriolis force;
- $\epsilon_h, \epsilon_v$  The horizontal and vertical eddy viscosity coefficients, which are estimated using Smagorinsky model:

$$\epsilon_h = C_h \Delta x \Delta y \left[ \left( \frac{\partial u}{\partial x} \right)^2 + \frac{1}{2} \left( \frac{\partial v}{\partial x} + \frac{\partial u}{\partial y} \right)^2 + \left( \frac{\partial v}{\partial y} \right)^2 \right]^{0.5} \quad (6)$$

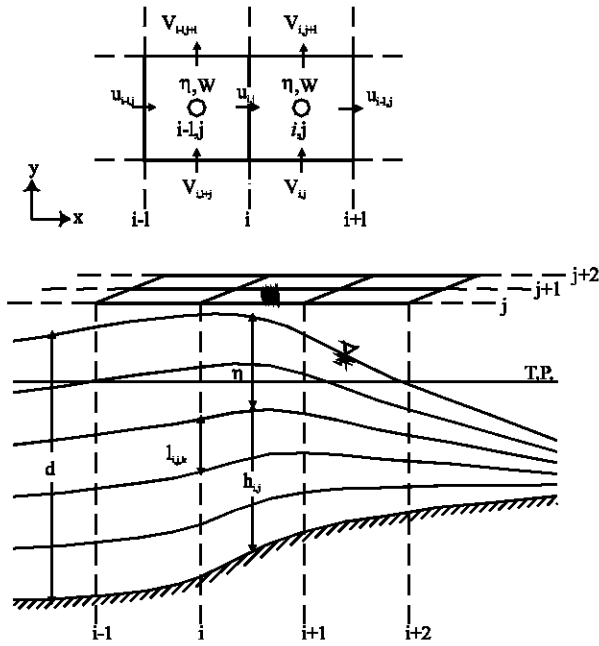


Fig. 1: Definition of space-staggered grid system

$$\epsilon_v = C_v \Delta z^2 \left[ \left( \frac{\partial u}{\partial z} \right)^2 + \left( \frac{\partial v}{\partial z} \right)^2 \right] \quad (7)$$

**Numerical solution:** The hydrodynamic equations were solved using the FSM, combining the finite difference method in the horizontal and the Finite Element Method (FEM) in the vertical, originally suggested by Koutitas and O' Connor (1980). This method is used for solving the equation of motion by dividing it into two differential sections and integrating at time separately for two stages. By using the FEM in the vertical direction, it can divide the water depth into equal layers and near sea-bottom layer is possible to divide finely. In this computation, the position of variables was defined using the space-staggered grid system (Fig. 1). Kuroiwa *et al.* (1998) has applied it to the Quasi-3D analysis of the nearshore currents.

The computational domain in the *x-y* plane is divided into a rectangular grid (Fig. 1). The vertical velocity and mean water level are computed at the center of each grid cell, whereas the horizontal velocity components are corrected midway along the cell faces. The mean water surface level for the next time step (*n+1*) is evaluated using the previous time step (*n-1*). Detailed description about open boundary conditions and implementation of wetting and drying are described in previous studies for the authors (Abualtayef *et al.*, 2006a,b).

**Boundary conditions:** The surface shear stresses due to wind are:

$$\left. \begin{aligned} \tau_{sx} &= \rho_a c_s W_x \sqrt{W_x^2 + W_y^2} \\ \tau_{sy} &= \rho_a c_s W_y \sqrt{W_x^2 + W_y^2} \end{aligned} \right\} (z = \eta) \quad (8)$$

where

$\rho_a$  The mass density of air;  
 $c_s$  The wind stress coefficient;  
 $W_x, W_y$  The wind speed components in *x* and *y* directions.

The bottom shear stresses are given by:

$$\epsilon_v \frac{\partial u}{\partial z} = \frac{\tau_{bx}}{\rho}, \epsilon_v \frac{\partial v}{\partial z} = \frac{\tau_{by}}{\rho}, (z = -h) \quad (9)$$

where  $\tau_{bx}$  and  $\tau_{by}$  are:

$$\left. \begin{aligned} \tau_{bx} &= \rho g u \sqrt{u^2 + v^2} / C^2 \\ \tau_{by} &= \rho g v \sqrt{u^2 + v^2} / C^2 \end{aligned} \right\} \quad (10)$$

The vertical velocity is given by

$$w = -u \frac{\partial h}{\partial x} - v \frac{\partial h}{\partial y} (z = -h) \quad (11)$$

### MODEL VERIFICATION

To prove the model accuracy and efficiency, the model is first tested against analytical solution for a standard case in a rectangular basin. The test was examined the vertical profile of horizontal velocity in a closed basin with a flat bed (2 km long × 2 km wide × 10 m deep) and with a non-slip bottom condition (Fig. 2). This experiment is concerned with the 3D uniform and steady state driven by wind forcing at the free surface. The analytical solution for the horizontal velocity component in a well-mixed channel with a known constant vertical eddy viscosity coefficient,  $\epsilon_v$  (Li and Zhan, 1993) is obtained:

$$u = \tau_{sx}^s \sigma (h + \eta) (3\sigma - 2) / 4\epsilon_v \rho, \sigma = (h + z) / (h + \eta) \quad (12)$$

where

$\tau_{sx}^s$  Surface wind stress;  
 $\rho$  Water density.

In this model run, a constant wind-induced stress is acted on the free surface. The simulations were performed

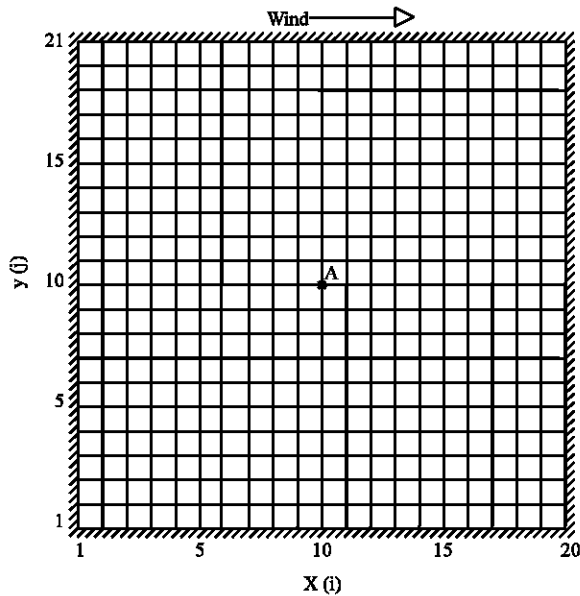


Fig. 2: Horizontal mesh used for simulation of wind-and tide-induced circulations

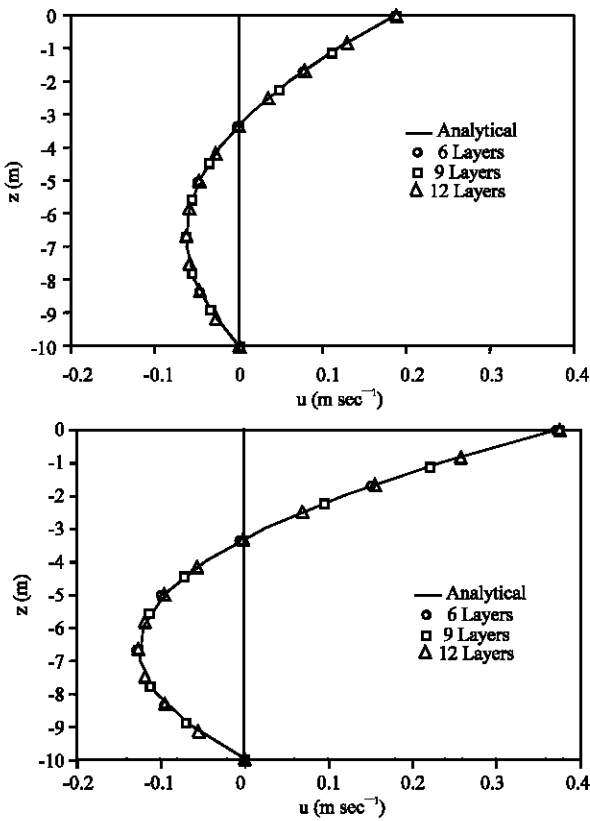


Fig. 3: Comparison of model-predicted velocity profile with analytic solution for wind driven flow in enclosed basin at point A for wind stress of (a)  $0.75 \text{ N m}^{-2}$  and (b)  $1.5 \text{ N m}^{-2}$

using 6, 9 and 12 layers, respectively; grid size is 100 m;  $\Delta t = 5 \text{ sec}$ ;  $\epsilon_v = 0.01 \text{ m}^2 \text{ sec}^{-1}$ ;  $\rho = 1000 \text{ kg m}^{-3}$  and Coriolis and horizontal diffusion terms were neglected. For this standard test case, two wind conditions were applied, where the wind stress was set to  $0.75$  and  $1.5 \text{ N m}^{-2}$ , respectively.

The model was started with a zero velocity and elevation and the simulation continued under constant wind force. The convergence is reached from cold start after the program is run for half period (6 h). Comparisons of model predictions at the center of the basin (at A as shown in Fig. 2) with the analytic solutions of vertical profile for u-velocity are shown in Fig. 3. It can be seen that the numerical solutions are almost identical to the analytical solutions, where the upper layer currents are in the wind direction while the lower layer currents are in the opposite direction, to maintain the mass balance in the

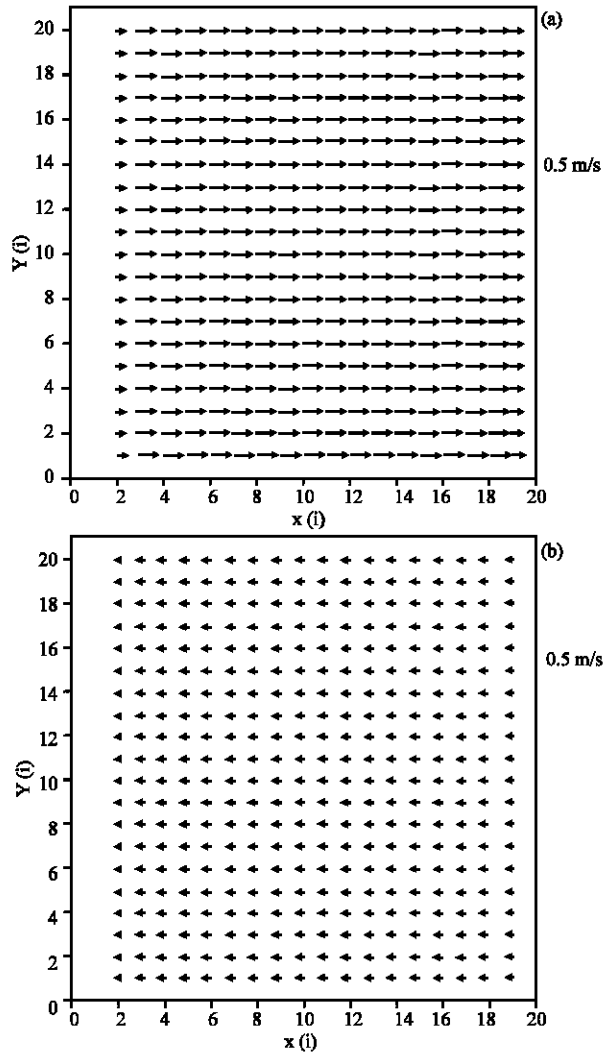


Fig. 4: Computed currents due to wind at (a) surface layer and (b) middle layer

closed basin. The maximum relative error of numerical and analytical velocities at free surface was decreasing by increasing the number of layers. The relative error for 6 layers model was 1.4 and 7% at surface layer and middle layer, respectively. And for 12 layers model, it was 0 and 2% at surface layer and middle layer, respectively. The flow velocities in the vertical direction change from a maximum value at the free surface to zero at about 3.3 m of the water depth and the flow direction then reverses below 3.3 m.

Figure 4 shows the computed wind-induced currents at surface and middle layers. It shows that the flow reverses their direction at lower layers.

**MODEL APPLICATION AND DISCUSSION**

As a practical case study, the Ariake Sea is a long inner bay with a complex bathymetry. It is located on the west of Kyushu Island, on the west part of Japan, which has an area of 1,700 km<sup>2</sup>, the extended 96 km of the bay axis, 18 km of the average width and 20 m in average depth. The model was applied to simulate the circulation patterns in the Ariake Sea. Figure 5 shows the water depth contour map of the study area.

Since we assume that there is neither current nor elevation in the sea initially, the calculated tide is a type of progressive wave in the early stage. Therefore, at least 4 periods of computations are required to get periodically stationary solution and only the computed results for the fourth period was taken and analyzed.

The horizontal computational domain covers an area of 81 km (NS) and 47 km (EW). A uniform Southerly wind speed of 7 m s<sup>-1</sup> was chosen as a representative direction. The wind was assumed to act over the whole modeling area. The water depth was divided into 5 equal layers. At the water level fluctuation type,  $\alpha$  is an incidence angle of the tidal wave in an open seaside boundary shown in Table 1 and  $k$  is the wave number, which was computed using of long wave theory.

Table 1: Computational conditions of the hydrodynamic model for Ariake sea

Contents	Values
Number of grids	162 [NS] x 94 [EW]
Grid size, = $\Delta x = \Delta y$	500 m
Water level	$\eta = -a \sin(ky \sin \alpha - \sigma t)$ , $\alpha = 0$
Coriolis parameter	$2\Omega \sin \varphi$ , $\varphi = 36.5^\circ$
$\epsilon_h$	$10 \text{ m}^2 \text{ sec}^{-1}$
$\epsilon_v$	$0.1 \text{ m}^2 \text{ sec}^{-1}$
Period, T	12 h
Amplitude, $\alpha$	1.08 m at open boundary
$\Delta t$	1.0 sec
Velocity of side boundary	$\partial u / \partial x = 0$ , $\partial v / \partial y = 0$

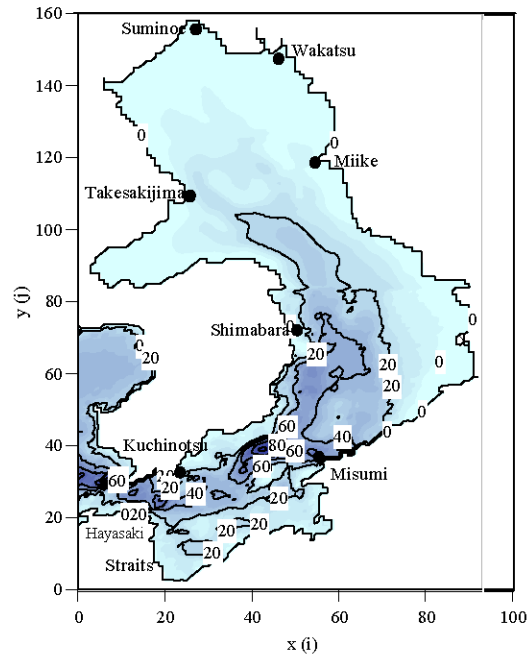


Fig. 5: Depth contour map of Ariake Sea

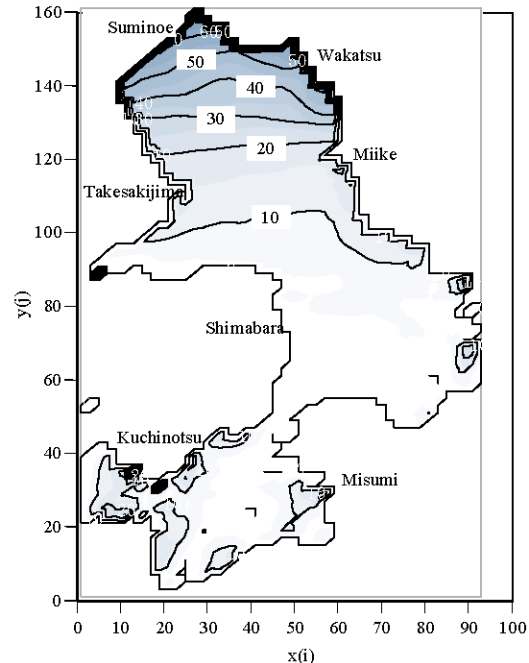


Fig. 6: Storm surge elevation contours (mm)

Tidal residuals may be caused by wind stress acting on the sea surface, inflow of fresh water, topographical influence, nonlinearity in tidal motion, etc. Taking these causes into consideration it will be inferred that tidal

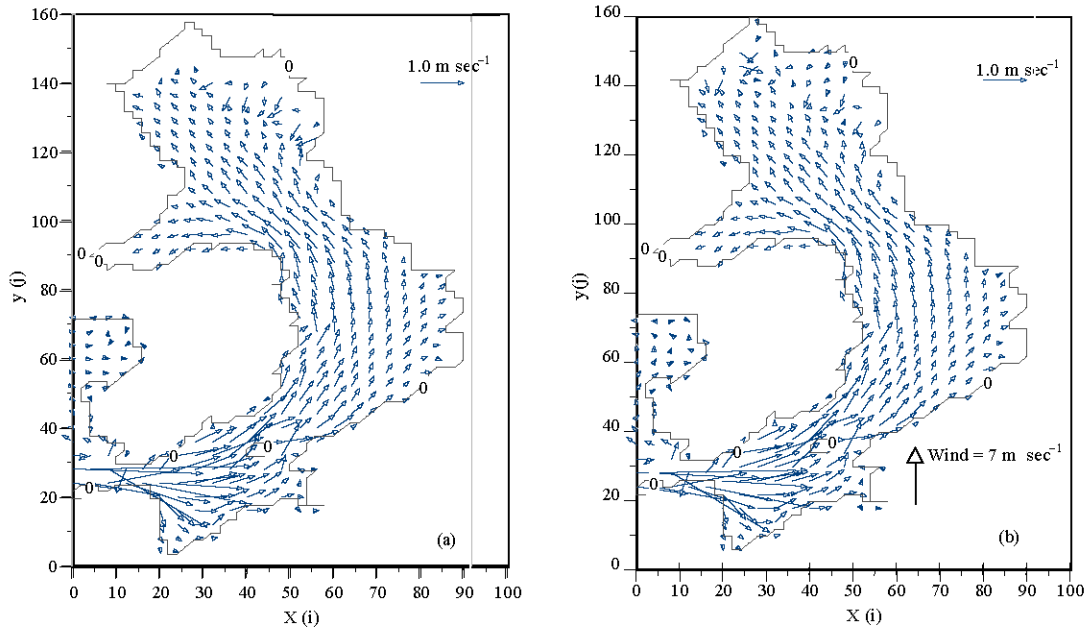


Fig. 7: Depth-averaged computed tidal currents in Ariake Sea with (a) no wind and (b) including South wind of  $7 \text{ m sec}^{-1}$

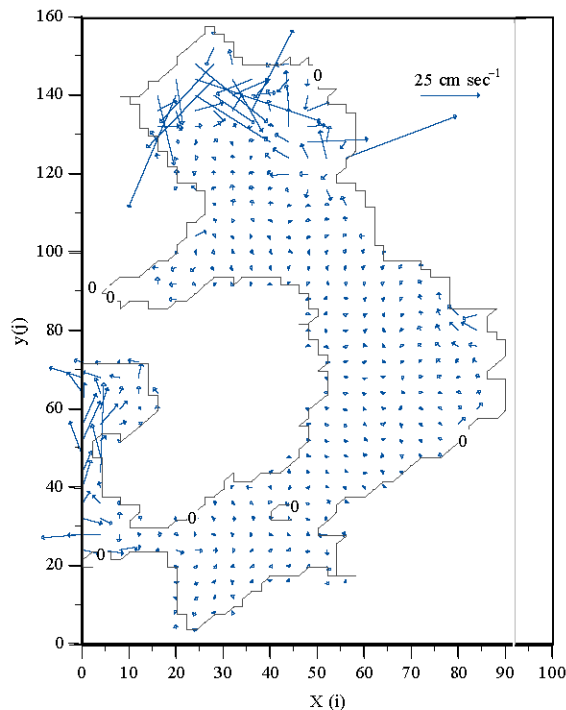


Fig. 8: Depth-averaged computed residual currents in Ariake Sea

residuals cannot organize universal circulation pattern, but reveal rather transient circulations (Isozaki and

Kitahara, 1977). Through this model, modification of tidal residual currents by wind stress acting on sea surface is examined.

Since the tidal currents in the region are strong (typically exceeding  $3 \text{ m sec}^{-1}$  at Hayasaki Straights and  $0.5\text{-}1.0 \text{ m sec}^{-1}$  in the middle and innermost part of the bay) as shown in Fig. 7. It is necessary to include the tide within the model since its current has a significant effect upon the level of turbulence. The storm surge elevation is presented in Fig. 6, which is gradually increasing at the northern bay. The results shown in this figure were calculated by considering the tide with and without the wind stress and the storm surge elevations are the difference between them.

The predicted depth-averaged tidal currents for strong flood are shown in Fig. 7 with (a) no wind and (b) Southerly wind. The residual currents due to wind stress were computed as the difference between these two conditions and plotted in Fig. 8. The fastest residual currents of more than  $0.5 \text{ m sec}^{-1}$  are seen near the bay head. We can conclude that the residual currents are very sensitive to shallow waters such as tidal flat.

## CONCLUSIONS

A 3D numerical model was developed to simulate the wind-induced circulations in the Ariake Sea. The model was tested against analytical solutions. The numerical

model predilections were found to be identical with the analytical results for the velocity structure over depth being well reproduced. Finally, the model was applied to Ariake Sea and the predicted residual currents were computed. The wind-induced circulation was found very sensitive to shallow waters such as tidal flats. Therefore, it should be considered in the modeling of tidal flat circulation. An appearance of the storm surge elevation over the tidal flat region was demonstrated clearly. For future work, further field observations are required for the study area, in order to investigate the circulation patterns and the sensitivity of the model parameters.

### REFERENCES

- Abualtayef, M., M. Kuroiwa, Y. Yamashita, K. Tanaka, Y. Matsubara and J. Nakahira, 2006a. Three dimensional numerical modeling of tidal currents in inter-tidal zone. *Int. J. Offshore Polar Eng., ISOPE.*, 16: 592-599.
- Abualtayef, M., M. Kuroiwa, K. Tanaka, Y. Matsubara and J. Nakahira, 2006b. Three dimensional numerical simulations of wetting and drying bed due to tidal currents using fractional step method. In: *Proceeding of 30th International Conference on Coastal Engineering*, ASCE (In Press).
- Casulli, V. and R.T. Cheng, 1992. Semi implicit finite-difference methods for three dimensional shallow water flow. *Int. J. Numerical Methods Fluids*, 15: 629-648.
- Caviglia, F.J. and W.C. Dragani, 1996. An improved 2-D finite-difference circulation model for tide-and wind-induced flows. *Comput. Geosci.*, 22: 1083-1096.
- Davies, A.M. and J.E. Jones, 1992. A three-dimensional wind driven circulation model of the Celtic and Irish Seas. *Continental Shelf Res.*, 12: 159-188.
- Elliott, A.J., 1986. Shear diffusion and the spread of oil in the surface layers of the North Sea. *Deutsche Hydrographische Zeitschrift*, 39: 113-137.
- Heaps, N.S., 1972. Estimation of density currents in the Liverpool Bay area of the Irish Sea. *Geophysical J. R. Astronomical Soc.*, 30: 415-432.
- Huai, Wen-xin, Y.P. Sheng and T. Komatsu, 2003. Hybrid finite analytic solutions of shallow water circulation. *Applied Math. Mech.*, 24: 1081-1088.
- Huntley, D.A. and A.J. Brown, 1990. Modeling Sand Transport on Continental Shelves. In: *Modeling Marine Systems*, Davies, A.M. (Ed.), CRC Press, Boca Raton, Florida, pp: 221-254.
- Isozaki, I. and E. Kitahara, 1977. Tides in the bays of Ariake and Yatsushiro. *The Oceanograph. Mag.*, 28: 1-32.
- Jin, X. and C. Kranenburg, 1993. Quasi-3D numerical modeling of shallow-water circulation. *J. Hydraulic Eng.*, ASCE, 119: 458-472.
- Kocyigit, M.B. and O. Kocyigit, 2004. Numerical study of wind-induced currents in enclosed homogeneous water bodies. *Turk. J. Eng. Enviorn. Sci.*, 28: 207-221.
- Koutitas, C. and B. O'Connor, 1980. Modeling 3D wind-induced flows. *J. Hydraulic Division, ASCE.*, 11: 1843-1865.
- Koutitas, C. and M. Gousidou-Koutita, 1986. A comparative study of three mathematical models for wind-generated circulation in coastal areas. *Coastal Eng.*, 10: 127-138.
- Kuroiwa, M., H. Noda and Y. Matsubara, 1998. Applicability of a quasi-3D numerical model to nearshore currents. In: *Proceeding of 26th International Conference on Coastal Engineering*, ASCE, pp: 2815-2827.
- Li, Y.S. and J.M. Zhan, 1993. An efficient three-dimensional semi-implicit element scheme for simulation of free surface flows. *Int. J. Num. Methods Fluids*, 16: 187-198.